

DYNAMIC LOADING METHODOLOGIES

*by Dr. Monty Moshier, Dr. Ronald Hinrichsen,
and Mr. Gregory J. Czarnecki*

It's becoming clear that current static loading techniques for live-fire testing fail to accurately replicate the loads of aircraft that are damaged in flight. Unfortunately, vulnerability assessments based on such loading techniques may also, in turn, fall short of providing accurate and complete results. The good news is advances in a proposed technique for dynamic live-fire ground testing may remedy the shortcomings of current static ground testing. And in response, the Joint Technical Coordinating Group on Aircraft Survivability (JTTCG/AS) is funding the Dynamic Loading Methodologies (DLM) program.

One aspect of the DLM program includes developing an exciting new strategy for more accurately testing in-flight damage to aircraft. In this article, we'll explore this promising new approach. But let's first identify the main shortfalls with static ground testing.

- Static stiffness is sufficient to withstand the aerodynamic loads (this assumes that sufficient lifting capability remains)
- Damage does not reduce the flutter speed such that the wing responds in a manner that it uncontrollably flutters and destroys itself.

In live-fire testing of aircraft wings, quasi-static ground loading techniques do not account for changes in structural stiffness and mass that occur from damage. As such, current loading methodologies fail to reconfigure correctly for representing in-flight loads. Ground loading methodologies also fail to consider damage-induced changes to the flutter envelope that can lead to premature failure.

What's needed is a different reconfigurable ground loading methodology that conforms to a wing's change in stiffness. And this must be combined with an analytical procedure that considers a wing's damage state and predicts a revised flutter envelope. Such a new ground loading procedure and complimentary flutter analysis will support live-fire testing and assist in generating reliable and complete test assessments and vulnerability analyses.

Defining a New Approach

Modeling and simulation, using a representative fighter aircraft model, helped us develop a new reconfigurable ground loading methodology to better predict the time response of an in-flight aircraft wing to damage. Our approach included—

- Obtain a validated finite element structural model and couple it with an aerodynamic flow model.
- Perform a time integrated finite element simulation of an in-flight aircraft. During the simulation, at ($t = 0$) apply the g-loading and aerodynamic loading to the model.
- Allow the model to come to a steady state condition.
- At a time when the model is at or near steady state ($t = t_1$) instantaneously inflict damage (equivalent to a specific threat) by removing structural elements from the model.
- Monitor the time history of displacements and strains at specific points in the model.
- Design a ground loading system to mimic the model response for the 1–2 seconds following the damage.

We obtained a finite element structural model of a representative fighter aircraft in NASTRAN format. This model had been previously validated for use in dynamic analysis and optimization. The NASTRAN model was translated into the LSDYNA3D format using a combination of MSC/PATRAN, FEMB, and user written translation codes. The resulting finite element model—consisting of 4,226 nodes, 2,016 beam elements, 4,984 shell elements, and 998 lumped masses and inertias—appears in Figure 1.

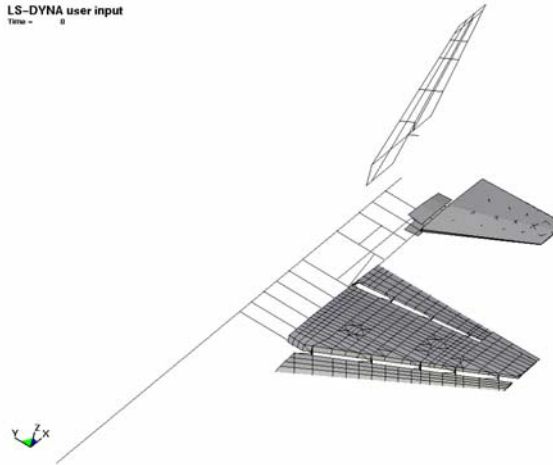


Figure 1. Structural Model

Because the focus of this work is on the wing, the highest fidelity elements were used there while other structures were modeled with less fidelity. The fuselage, vertical, and horizontal tails are essentially beam models.

The aerodynamic paneling model used was a boundary element method based on the VSAERO code and appears in Figure 2.

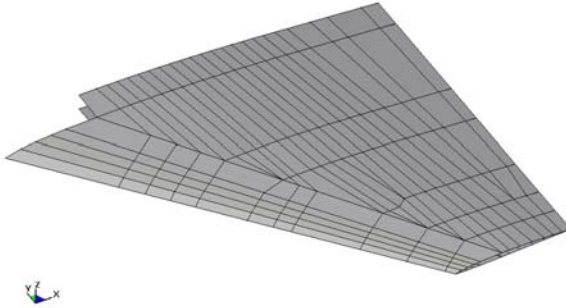


Figure 2. Aerodynamic Panel Model

Because the model is based on linear aerodynamic theory, it's applicable for inviscid, incompressible fluid flows. It consists of 336 elements using nodes that are coincident with and numbered the same as the structural model nodes. By imposing the coincidence of the aero and structural nodes, pressures generated by the aero model are directly applied to the structural nodes.

The coupled aero/structural model assumes symmetry about the centerline of the aircraft with the structure fixed at the center of mass of the symmetric model.

Revalidating the Model

After the NASTRAN finite element model of the structure was converted to LSDYNA3D format, we needed to revalidate the new model. We achieved this by comparing the performance of the two models against existing data that had been obtained from earlier static and dynamic ground tests.

- **Static validation**—the new LSDYNA3D model displacement was quite sensitive to the imposition of the cantilevered boundary condition. When compared to the original NASTRAN model, the LSDYNA3D was significantly better, depicting a displacement about 5 percent greater than ground test.

- **Dynamic validation**—due to the explicit nature of the LSDYNA3D code, natural frequencies were determined in the time domain by cantilevering the wing model at the root and “plucking” the wing tip. The time history of displacement in the z direction of selected nodes was extracted and a fast fourier transform (FFT) was applied to obtain the frequency response. The difference between the LSDYNA3D model and the ground test values varied between 6% and 16%.

Using this validated, coupled aerodynamic/structural finite element model, let's now explore the results of three sample simulations.

Simulating Dynamic Response to In-Flight Damage

The results we'll discuss are from simulations in which the wing was undamaged for the first 10 seconds with instantaneous damage to the wing occurring at $t=10$ seconds followed by an additional 10 seconds of simulation.

The aerodynamic paneling method used in LSDYNA3D does not currently allow for ramping up of the aerodynamic flow. Because of this, the initial 10 seconds of simulation is required, allowing the wing's response to the step loading from the aerodynamic flow to reach a steady state. Instantaneous damage to the wing at $t=10$ seconds is achieved by removing

elements associated with the assumed damage. The resulting dynamic response from the damage and applied aerodynamic loading is then captured in the final 10 seconds of the simulation. The aerodynamic mesh does not change throughout the simulation.

Sample Case 1—Clean Wing Damaged (Moderate) Near The Wing Root

The model simulation was for the aircraft at an angle of attack of 6 degrees, altitude below 4,000 feet and mach 0.8 (see Figure 3).

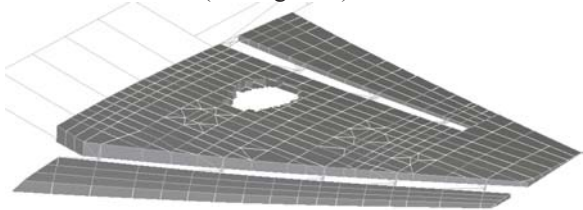


Figure 3. Sample Case 1. Typical Damage – Mach 0.80

This case illustrates this particular wing's structural redundancy. After the wing reaches steady state, aerodynamic loading causes the undamaged wing to deflect approximately 3.5 inches, as measured from B.L. 120 (see Figure 4).

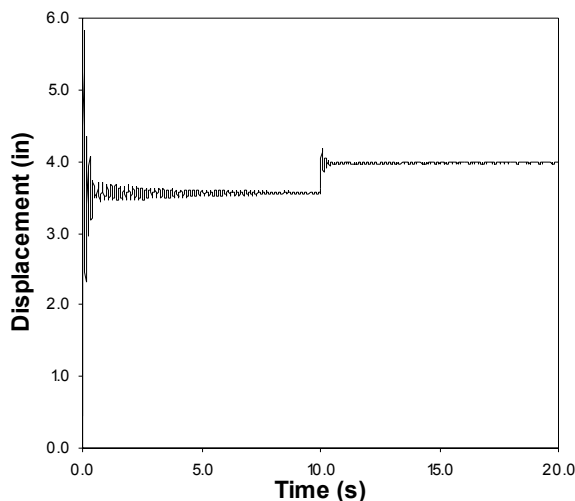


Figure 4. Deflection at B.L. 120 For a Clean Wing and Typical Damage – Mach 0.80

The above chart also shows that once damage occurs, the instantaneous loss of structural stiffness initiates some brief oscillations

followed by a steady state deflection that is approximately 0.5 inches more than the predamage state.

Under these simulated flight conditions, the wing's reduction of stiffness due to damage doesn't affect the dynamic response of the wing sufficiently to cause catastrophic failure. However, brief oscillations experienced immediately following damage, under the right conditions, may cause additional damage that results in additional stiffness loss, that may propagate.

Let's take a look at this wing's redundancy by examining stresses in the damaged spar caps. As shown in Figure 5, spar cap stresses exist in spar caps 6 and 7 before and after damage.

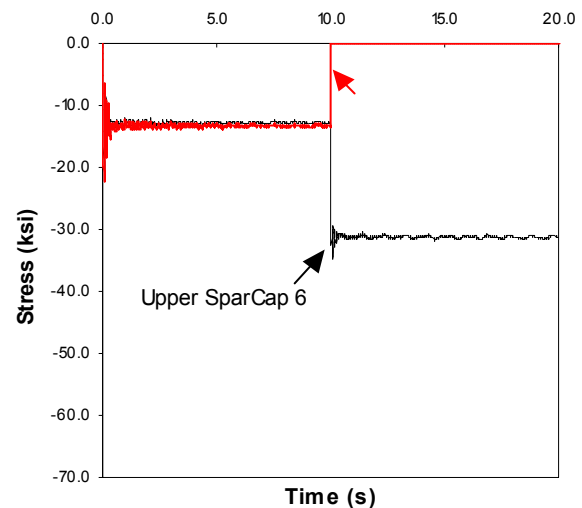


Figure 5. Spar Cap Stresses Before And After Damage

Portions of spar cap 7, 8, 9, and 10 are eliminated at time $t=10$ seconds. Before damage is input, spar caps 6 and 7 are loaded to about 12 ksi. After damage, spar cap 6 is loaded to 30 ksi because it carries additional load from the damaged spar caps. The yield stress of aluminum used in modeling the spar caps is 70 ksi. As can be seen, the post-damage stresses are far below the allowable yield.



Figure 6. Wing Deflection With Typical Damage And Wing Tip Store – Mach = 0.92

Sample Case 2—Clean Wing Damaged (Moderate) Near The Wing Root With A 300 Pound Store Attached To The Wing Tip

This model simulation was for the aircraft at an angle of attack of 3 degrees, altitude below 4,000 feet and mach 0.92. The 300 pound store was modeled as a series of simple beams.

This case (see Figure 7) illustrates the wing's deflection and tortuous shape caused by the damage and reduced flutter resistance.

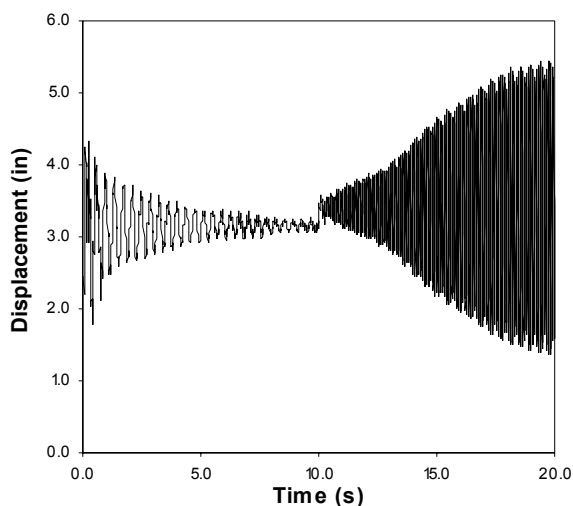


Figure 7. Deflection At B.L. 120 For Wing + 300lb. Store And Typical Damage – Mach = 0.92

In this case, the oscillations associated with step loading the wing at the beginning of the simulation require more time to reach steady state than the previous case. After damage, the deflection diverges due to the lower stiffness and reduced flutter speed. The reduced flutter resistance caused by the damage led to increased

deflections resulting in stresses that exceed the allowable yield stresses of the materials used.

You can compare the Von Mises stresses for this wing prior to damage and after damage in the following illustrations. In these illustrations the Von Mises stresses are scaled such that blue is 0 ksi and red 70 ksi, corresponding to the maximum allowable yield stress. Before damage the Von Mises stresses were all well below the yield stresses (see Figure 8) and after damage due to the increased deflections caused by flutter, the Von Mises stresses exceeded the allowable yield stress in the entire tip region (see Figure 9).

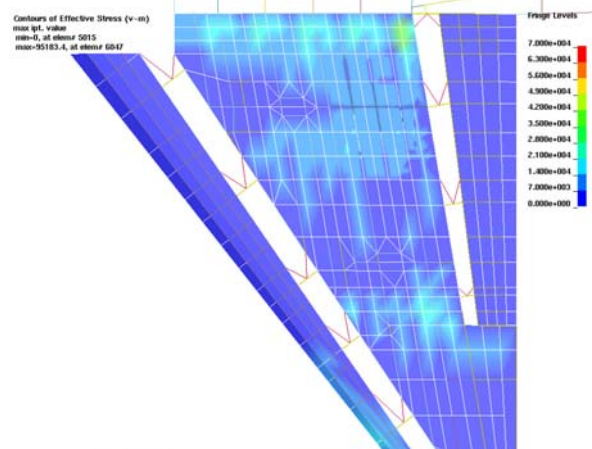


Figure 8. Von Mises Stress Contour Plot For Wing Just Before Damage

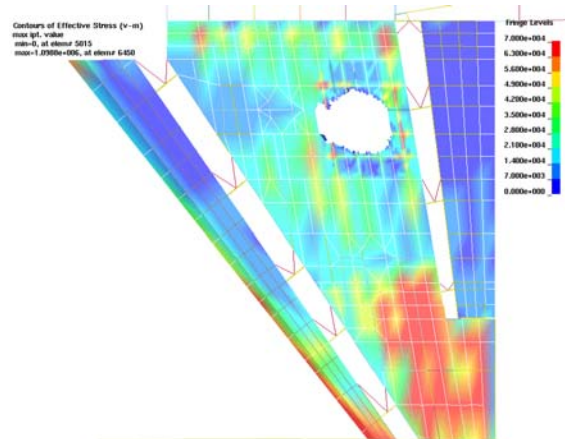


Figure 9. Von Mises Stress Contour Plot For Wing After Damage

The likely result would be the loss of the wing tip and possible loss of the aircraft.

Sample Case 3—Dynamic Response Of A Clean Wing Damaged Near The Wing Tip

This model simulation was for the aircraft at an angle of attack of 3 degrees, altitude below 4,000 ft., and mach = 0.95 (see Figure 10).

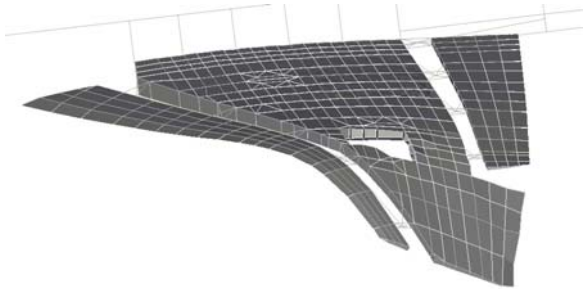


Figure 10. Wing Deflection With Typical Wing Tip Damage – Mach = 0.95

This case illustrates how damage causes severe wing distortion. After damage, the tip deflections have an oscillation of 50 inches (see Figure 11).

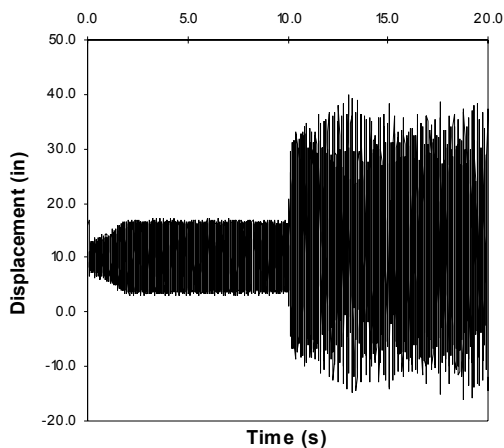


Figure 11. Deflection Of Wing Tip -- Typical Damage Located Near Wing Tip – Mach = 0.95

Before damage, the oscillations are a factor of 5 smaller. Note: the deflections presented are given at the wing tip and not at B.L. 120 as in the previous two cases. In this case, deflections at B.L. 120 were much less severe since the damage occurred outside of B.L. 120.

Now compare the Von Mises stresses for this wing before and after damage, respectively. Again, Von Mises stresses are scaled such that blue is 0 ksi and red is 70 ksi, with red

corresponding to maximum allowable yield stress.

Before damage the Von Mises stresses are within the allowable range (see Figure 12) while stresses after damage are above the allowable for most of the wing (see Figure 13).

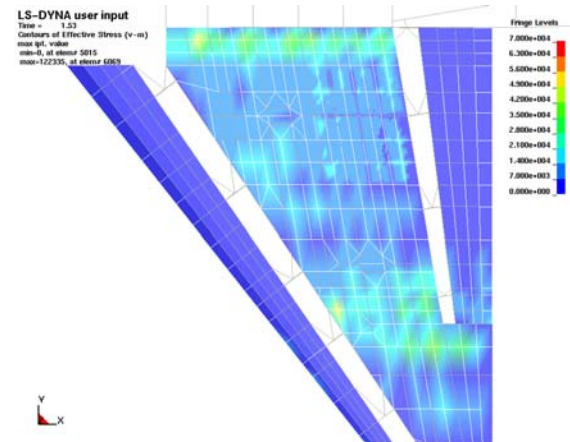


Figure 12. Von Mises Stress Contour Plot For Wing Before Damage

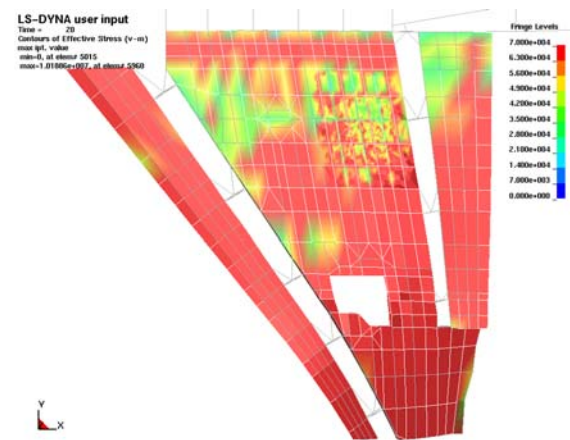


Figure 13. Von Mises Stress Contour Plot For Wing After Damage

The obvious result from this simulation would be loss of the wing and aircraft, unless flight conditions were modified.

Planning Next Steps

Because of the nature and use of fighter aircraft, several different conditions, such as the effect of different stores, flight conditions, damage locations, and size, must be considered to better understand the wing's dynamic response when damaged. Beyond the three cases just shown,

this DLM program investigated over 68 cases in which stores ranged from 200 to 2,000 pounds; flight conditions ranged from mach 0.8 to mach 0.95 below altitudes of 4,000 feet; and damage included three different damage sites and two different damage sizes.

We're pursuing the strategy discussed in this article to more faithfully represent the structural response of in-flight aircraft to damage. But we also understand the limitations of the aerodynamic model being used.

For example, the dominant source of damping in these simulations was due to the aerodynamics alone. No structural damping was added. Some numerical damping was present to ensure stability of the solutions, estimated to be less than 1% of that induced by the aerodynamics. No unsteady aerodynamics were modeled. The linear, incompressible, inviscid assumptions associated with the paneling method limit applicability of these analyses to subsonic conditions. Also, a linear material model was used for all materials.

Because of these limitations, Professor Charbel Farhat and his team at the University of Colorado are conducting an independent blind study. That team is using a Navier-Stokes CFD model for the aerodynamics. The goal is to quantify differences obtained by the two methods. The intent is to use the fidelity of model appropriate for the flight condition of interest.

The team is investigating possible pneumatic, hydraulic, or combined loading techniques that could be used to apply dynamic loads during ground tests. It is anticipated that experimental ground testing can be applied for cases similar to case 1. The simulations have shown that the dynamic response and flutter resistance based on cases similar to that of case 2 and 3 results in deflections that if applied to an actual wing would lead to structural failure. Therefore, when flutter plays a key role in the dynamic response of the wing due to damage (cases 2 & 3), it's anticipated that computational analyses will be used as the primary tool for accurately assessing post-damage survivability.

As this article demonstrates, modeling plays a key role in determining appropriate loading methods for likelihood of aircraft survivability. But a full structural evaluation should account

for more than just a maximum yield stress criterion as was done here. Many other failure mechanisms from plasticity to cracking must also be considered.

Planned future work in this promising area will yield additional results of dynamic analysis. These results, in turn, will help provide a pathway to test engineers for determining the most appropriate test method. That method could either be static, dynamic, or a combination of the two. And the good news there, is that subsequent concept designs of dynamic ground tests may then be based on improved predicted structural response.

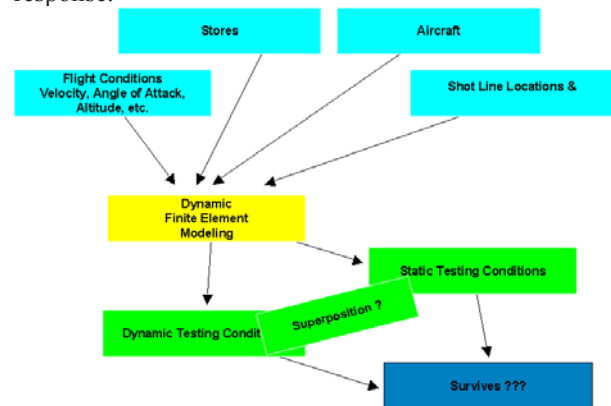


Figure 14. Proposed Dynamic Loading Methodology Strategy

Dr. Monty Moshier received his Ph.D. in Mechanical Engineering from Purdue University. He is a Senior Scientist at RHAMM Technologies, LLC. He may be reached at moshier@rhamm.com.

Dr. Ronald Hinrichsen received his Ph.D. in Aeronautical Engineering from the Air Force Institute of Technology. He is currently a Senior Research Scientist at NCSA, Univ. of Ill. He may be reached at hinricrl@asc.hpc.mil.

Mr. Czarnecki received his B.S. in Civil Engineering and his M.S. in Materials Engineering from the University of Dayton. He is a civilian with the Air Force Research Laboratory Air Vehicles Directorate, Survivability & Safety Branch. He may be reached at Gregory.czarnecki@wpafb.af.mil